The International Journal of Advanced Manufacturing Technology (2019) 103:367–376
https://doi.org/10.1007/s00170-019-03560-1

ORIGINAL ARTICLE

Impact of a process interruption on tensile properties of SS 316L parts and hybrid parts produced with selective laser melting

Philipp Stoll[1] · Adriaan Spierings[1] · Konrad Wegener[2]

Received: 11 January 2019 / Accepted: 8 March 2019 / Published online: 20 March 2019

Abstract
Selective laser melting (SLM) facilitates the integration of external elements like sensors into workpieces during manufacturing. These embedded components enable, e.g., part monitoring thus being a fundamental application of industry 4.0 and digitization of products in general. Since these embedding concepts are currently developing, the research community focusses on survival, functionality, and data quality of the embedded elements. However, another important aspect is that the manufacturing processes need to be interrupted for sensor integration. This study investigates the influence of a process interruption on the static tensile properties. The results reveal a distinct impact of the process discontinuity on the tensile properties. Both yield strength $R_{p0.2}$ and ultimate tensile strength R_m dropped by 13% for horizontally orientated tensile bars and by 18% for vertical samples. True stress for both horizontal and vertical samples is also negatively affected by the process interruption. Furthermore, hybrid tensile bars that consist of half conventionally and half additively manufactured parts were tested since this manufacturing approach also implies a start of the SLM process within the final part's shape. For these samples, true stress and plastic strain values represent an even mix between vertical and conventional tensile bars. For all samples, the location of failure was analyzed by fractographic and cross-sectional analyses. For the SLM samples, the process interruption represents a potential weakening of the cross section, even though not all samples broke in the interruption zone. The hybrid tensile bars did not fail in the transition zone, which consequently is not the weak spot of these samples.

Keywords Selective laser melting (SLM) · Hybrid parts · Sensor integration · Embedding · Tensile properties · Industry 4.0

1 Introduction

Selective laser melting (SLM) is an additive manufacturing (AM) technology that currently receives more and more attention in production industry. It offers new possibilities and strategies for the manufacturing of functional metallic parts. The main benefits of SLM compared with conventional manufacturing technologies are the possibility to design and produce parts based on their core functional purposes, and not hampered by the restrictions and limitations of traditional manufacturing. Additionally, it enables the production of highly complex shapes. This results in parts typically exhibiting complex design features, bionic inspired shapes, or topology optimized lightweight structures that are of enormous interest for various industrial sectors. Furthermore, due to the layer by layer process SLM facilitates the integration of functional elements like sensors into the workpieces during their manufacturing. This is a promising approach for numerous applications since the sensors can be placed in immediate vicinity of the locations of interest, e.g., where a signal needs to be monitored. Paz [1] as well as Sehrt and Witt [2] investigated the integration of RFID tags into components during the SLM production process, while Stoll [3] demonstrated the functional embedding of Pt 100 temperature sensors in 316L stainless steel (SS 316L) parts. For high temperature sensing, optical fibers are embedded during manufacturing. Optical fibers are the type of sensor whose integration during manufacturing has been investigated the most. Based on the work of Li [4] who presented an approach to embed optical fibers in additively manufactured parts by means of direct metal deposition (DMD), lately many papers

✉ Philipp Stoll
stoll@inspire.ethz.ch

[1] Inspire, Innovation Center for Additive Manufacturing Switzerland (icams), Lerchenfeldstrasse 3, 9014 St. Gallen, Switzerland

[2] Institute of Machine Tools and Manufacturing (IWF), Swiss Federal Institute of Technology, ETH Zürich, Leonhardstrasse 21, 8092 Zürich, Switzerland

about integration of optical fibers into SLM parts have been published. Maier [5] reported the direct integration of metallic jacketed fibers into stainless steel coupons on a SLM test setup. Havermann [6, 7] focused on the description of the fiber embedding strategy for the aforementioned SLM test setup. Furthermore, he analyzed the influences of various process parameters on the embedding procedure and the corresponding bonding qualities between the optical fiber and the surrounding material. Finally, Stoll [8] has been able to transfer the process steps for fiber integration from a lab SLM test setup to a commercial SLM system. All the earlier work focused on the integration and functionality of the various types of sensors after embedding which is a very important first step in developing embedding strategies. Another aspect that is inherently linked to sensor embedding during SLM manufacturing is the interruption of the SLM process which might have an impact on the mechanical properties of the manufactured parts since it leads to a discontinuity in the formation of the part. Though embedding external components into SLM parts is not the only manufacturing procedure facing a process interruption. As SLM is evolving rapidly from prototyping to a serial production technology, cost effectiveness as well as productivity is becoming more and more important. Consequently, hybrid parts, manufactured by combining traditional machining for bulky and geometrically simple parts and additive manufacturing for the production of complex structures containing added value, raise interest in industry. However, the influence of the SLM process interruption and of the transition zone between conventional and additive manufacturing of the same material for hybrid parts has not yet been discussed in any research papers. Therefore, this paper investigates the impact of a SLM process interruption on static mechanical properties of SS 316L. Furthermore, the mechanical properties of hybrid tensile bars are presented and discussed. The results allow to quantitatively assess the manufacturing concepts described above and enable their industrial realization and implementation.

2 Materials and methods

2.1 Material and SLM machine

A Concept Laser M2-machine equipped with a Nd:YAG laser with 1064 nm wavelength and maximum power of 400 W operating in cw-mode was used for the manufacturing of test samples. A process parameter set operating in islands scanning strategy and providing a volume energy density E_{vol} = 59.3 J/mm^3 according to commonly used following definition was used,

$$E_{vol} = \frac{P_{\text{Laser}}}{v_{\text{scan}} * h * t}$$

with laser power P_{Laser} = 180 W, scan speed v_{scan} = 1350 mm/s, hatch distance h = 75 μm, layer thickness t = 30 μm, and a laser spot diameter of 144 μm. The build chamber was filled with N_2 with an upper O_2 limit of 0.3%. This process parameter set led to a relative part density > 99.0% determined by Archimedes' principle compared with the reference value of 7.95 g/cm^3 given in the material certification provided by the powder deliverer Carpenter Powder Products. The gas atomized SS 316L powder used had a particle size distribution of d_{10} = 10.8 μm, d_{50} = 20.0 μm, and d_{90} = 37.0 μm.

2.2 SLM manufacturing of test specimens

For the assessment of the impact of SLM process interruption on mechanical properties, different batches of tensile bars according to DIN 50125 A5x25 were produced in horizontal and vertical build orientation, as depicted in Fig. 1 with z representing the SLM build-up direction. Table 1 gives an overview of the various batches, each composed of five tensile bars. The benchmark regarding mechanical properties was defined by tensile bars built in one step, i.e., without any SLM process interruptions, represented by V_0 and H_0 (Table 1). These values were compared with tensile bars that have been manufactured in two steps meaning the SLM process has been interrupted at the medium height of the specimens. This process interruption lasted minimal 60 min ensuring that the parts as well as the powder bed had cooled down to room temperature. Furthermore, during the interruption the machine was opened, i.e., the parts were in direct contact with ambient air. Figure 1 schematically shows the positions of the SLM process interruptions for the different build orientations. V_1 and H_1 represent batches where the SLM process has been continued in the standard way for the Concept Laser M2-machine, which means that the interruption surface has been scanned one time before a new powder layer has been applied. For the batches V_2 and H_2, the restart of the SLM process has been changed in that way that the interruption surface has

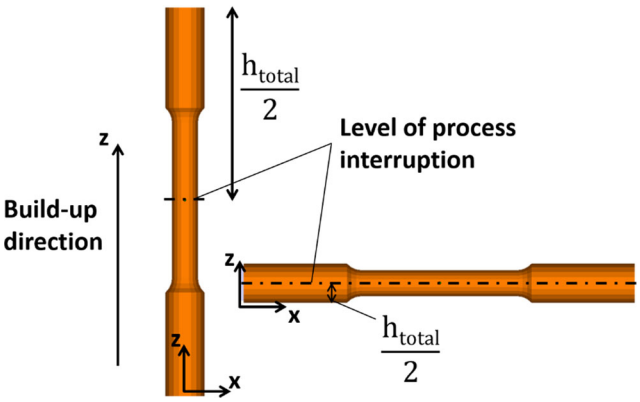

Fig. 1 Orientation of tensile bars with respect to SLM build-up direction z; Level of SLM process interruption for vertically and horizontally orientated tensile bars respectively

Table 1 Different processing strategies for SLM manufacturing of tensile bars

Batch-ID		V_0	V_1	V_2	H_0	H_1	H_2	X_1	X_2
Build orientation	Vertical	x	x	x				x	x
	Horizontal				x	x	x		
SLM procedure	Standard process	x			x				
	Process interruption		x	x		x	x		
	Hybrid parts							x	x
SLM process continuation	Standard		x			x			
	2 additional scans prior to process continuation			x			x		
Pre-processing of turned parts	No pre-processing							x	
	Shot-peening								x

been scanned three times before the first powder layer has been applied. With this additional variation, the influence of a higher energy input on the interruption surface shall be analyzed. Batches X_1 and X_2 consist of hybrid tensile bars manufactured in vertical orientation. Therefore, the lower half of the part had been conventionally manufactured from SS 316L bulk material in solution-annealed condition delivered by HABA AG [9]. Subsequently, the SLM process started on top of these parts. In batch X_1, the turned parts were used in their as manufactured condition, while an additional shot peening process step had been applied for the parts in batch X_2 prior to the start of the SLM process to create a surface structure which enables the application of a stable powder layer as it is usually done with the top surface of the substrate prior to the start of the SLM process. For all batches, the tensile bars were manufactured in a cylindrical shape while the final specimen geometry (Fig. 1) was achieved by a post-process turning operation. All batches were tested in the as-built by SLM condition, i.e., no heat treatment process was applied.

2.3 Analyses

The relative part density of the SLM samples was determined based on cube samples that were manufactured in the same build jobs as the tensile bars respectively. The measurement was conducted according to Archimedes' principle on an AX205 analytical balance from Mettler Toledo according to the procedure described by Spierings [10]. The static mechanical data was determined according to DIN EN-10002 (ISO-6892) on a LFV25 tensile testing machine from Walter and Bai. For the statistical evaluation of this data, a level of significance of $\alpha = 5\%$ was applied. Microstructural analyses were performed on ground and polished samples using a Bühler Phoenix 4000 machine and finally etched with V2A etchant for 30 s. The microscopic evaluation of the tensile bars' microstructure and fracture surfaces was done on a Leica DM6 M microscope and a FEI Quanta 200F scanning electron microscope (SEM).

3 Results and discussion

3.1 Static mechanical properties

The tensile testing results are displayed in Fig. 2 and summarized in Table 2. The data reveal clearly that for $\alpha = 5\%$ there is a statistically significant drop in the mechanical properties if the SLM process is interrupted: For the vertical samples, yield strength $R_{p0.2}$ drops by 18.5%, ultimate tensile strength R_m by 17.5% compared with the reference sample V_0. For the horizontal samples, the decrease is 13% for $R_{p0.2}$ and 11.5% for R_m. Furthermore, an anisotropic material characteristic is observed, and both $R_{p0.2}$ and R_m of the horizontal samples H_0, H_1, and H_2 are higher compared with the values of the correspondent vertical samples V_0, V_1, and V_2. The hybrid samples X_1 and X_2 have very similar R_m values as V_1 and V_2, with only 0.8% deviation, while the $R_{p0.2}$ values are 57.2% lower than those of V_1, V_2 and 15.1% higher than those of conventional SS 316L material. The bar charts in Fig. 2 (a) illustrate a very similar characteristic of batches that have been produced in a similar way, like V_1 compared with V_2, H_1 compared with H_2, and X_1 compared with X_2.

The anisotropic results of the tensile testing shown in Fig. 2 and Table 2 reveal a typical characteristic of the SLM process, which is widely reported by Levy [11], Mertens [12], Mower [13], Riemer [14], Spierings [15], and Hitzler [16] (Table 3). However, even the low values of V_0 compared with H_0 fit well into the range of tensile properties reported in scientific literature and outplay the properties of conventionally processed SS 316L, reported with $R_{p0.2} = 200$ MPa, $R_m = 500$–700 MPa in the supplier's datasheet [9], and experimentally verified with $R_{p0.2} = 264 \pm 4$ MPa, $R_m = 586 \pm 4$ MPa. The described larger influence of the process interruption on $R_{p0.2}$ and R_m of the vertical samples can be explained by the orientation of the interruption plane relative to the load during tensile testing. For the vertical batches, this plane is perpendicular to the applied force. Additionally, the interruption plane for the vertical samples lies exactly in the middle of the gage length, which is the region of elongation and potentially also of

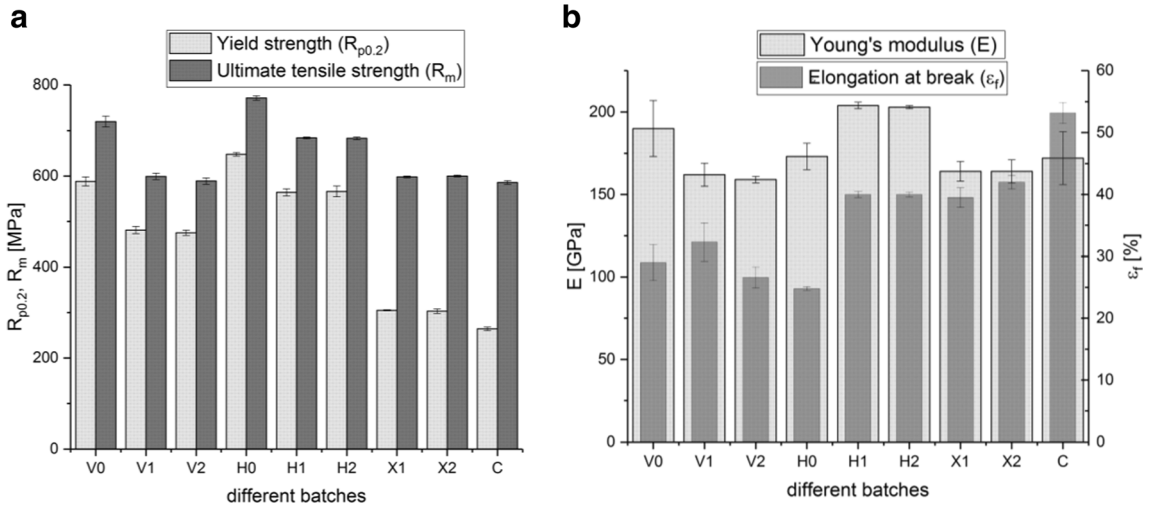

Fig. 2 Static mechanical properties of various batches of tensile bars. Yield strength $R_{p0.2}$ and ultimate tensile strength R_m (**a**). Young's modulus E and elongation at break ε_f (**b**)

necking. Since these two aspects do not apply for the horizontal batches, the decrease in $R_{p0.2}$ and R_m induced by the SLM process interruption is larger for the vertical samples. Among each other, the data of V_1 and V_2 are very similar, which means that the different restarting procedures of the SLM process after the interruption do not have a strong impact on the mechanical properties. The horizontal batches H_1 and H_2 do not reveal statistically significant differences in $R_{p0.2}$ and R_m, which leads to the same conclusion as for the vertical ones, that the different restarting procedures do not impact the mechanical properties. The hybrid manufactured batches X_1 and X_2 do not have a process interruption as the other samples, but the situation is comparable since there is a start of the SLM process within the final part's shape. This contact layer of conventionally and additively processed SS 316L is a discontinuity in the microstructure and consequently also in the mechanical properties. Therefore, the characteristic of the hybrid samples is a mix of conventionally and additively processed material. $R_{p0.2}$ is low compared with the other SLM processed batches but still representing the value of conventionally processed SS 316L. However, R_m is in the range of additively manufactured tensile bars with process interruption (V_1 and V_2). The data of X_1 and X_2 are very consistent and similar among each other which lead to the conclusion that the different pre-processing steps have no statistically significant impact on the mechanical properties.

For the elongation at break ε_f, the anisotropic behavior between horizontally and vertically orientated tensile bars cannot be observed. While batch H_0 has the lowest elongation at break of all batches ($24.8 \pm 0.3\%$), H_1 and H_2 reveal higher values than the vertical samples. ε_f of X_1 and X_2 is with a mean value of $41.3 \pm 1.6\%$ in a similar range compared with H_1, H_2 (mean of $\varepsilon_f = 39.8 \pm 0.5\%$), and exceeding V_1, V_2 (mean of $\varepsilon_f = 29.5 \pm 3.8\%$) considerably. ε_f (V_0) is with 29.0% well within the range of ε_f (V_1) = 32.3% and ε_f (V_2) = 26.6%, thus not showing any trend or impact of the process interruption on the elongation at break, but the standard deviations are considerably larger than for the horizontal batches. These batches however show a statistically significant difference between H_0 and H_1, H_2. ε_f increased from 24.8% (H_0) to 40% (H_1, H_2) with standard deviations between 0.3 and 0.5%. Since the results of H_1 and H_2 are nearly identical, it can be concluded that the two different SLM process restarting procedures for H_1 and H_2 do not have any impact on ε_f. The fact that there is no clear anisotropic behavior in the elongation at break between vertically and horizontally orientated specimens is also discussed in literature. While Hitzler [16] reported for additively processed SS 316L $\varepsilon_f = 43\%$ for horizontal tensile bars

Table 2 Yield strength $R_{p0.2}$, ultimate tensile strength R_m, elongation at break ε_f, and Young's modulus E for various batches of tensile bars according to Table 1

Batch	V_0	V_1	V_2	H_0	H_1	H_2	X_1	X_2	C
$R_{p0.2}$ [MPa]	588 ± 10	481 ± 8	475 ± 6	648 ± 4	564 ± 8	566 ± 12	305 ± 1	303 ± 5	264 ± 4
R_m [MPa]	720 ± 12	599 ± 7	589 ± 7	772 ± 5	684 ± 2	683 ± 3	598 ± 2	600 ± 2	586 ± 4
ε_f [%]	29.0 ± 2.9	32.3 ± 3.1	26.6 ± 1.7	24.8 ± 0.3	40.0 ± 0.5	40.0 ± 0.4	39.5 ± 1.6	42.0 ± 1.1	53.2 ± 1.7
E [GPa]	190 ± 17	162 ± 7	159 ± 2	173 ± 8	204 ± 2	203 ± 1	164 ± 6	164 ± 7	172 ± 16

C, conventionally processed SS 316L

Table 3 Tensile properties of SLM processed SS 316L—literature review

Literature reference	$R_{p0.2}$ [MPa]	R_m [MPa]	ε_f [%]
Mertens [12] vertical/horizontal samples	450/530	570/660	8/16
Mower [13]	496	717	28
Spierings [15]	640	760	30
Riemer [14]	462	565	53.7
Hitzler [16] vertical/horizontal samples	470/530	520/640	18/43

and only $\varepsilon_f = 18\%$ for vertical ones, Merkt [17] presented contrary results with $\varepsilon_f > 30\%$ for horizontal and $\varepsilon_f > 60\%$ for vertical specimens. ε_f of the hybrid specimens, which are vertically orientated, is with values of 39.5% and 42.0% in the same magnitude as the one of the horizontal samples with process interruption ($\varepsilon_f(H_1) = \varepsilon_f(H_2) = 40.0\%$) but has larger standard deviations. Since the two batches X_1 ($\varepsilon_f = 39.5 \pm 1.6\%$) and X_2 ($\varepsilon_f = 42.0 \pm 1.1\%$) do statistically not differ significantly, it can be stated that the different pre-processing steps did not affect the results. ε_f of the conventional tensile bars is with $53.2 \pm 1.7\%$ considerably larger than for all additively manufactured samples.

Regarding the Young's modulus E a very similar material behavior among batches from the same type can be observed: V_1 compared with V_2, H_1 compared with H_2, X_1 compared with X_2. However, the Young's modulus shows no systematic characteristic or anisotropic behavior, while V_1 and V_2 have lower values than the vertical reference batch V_0, this behavior is the other way round for the horizontal samples: E of H_0 is clearly lower than the one of H_1 and H_2 respectively. E of V_1 and V_2 is very similar to the values of X_1 and X_2.

3.2 Plastic deformation

Figure 3 shows the plastic deformation behavior for the various batches for the regions of uniform elongation in the tensile test, i.e., the end of the curves marks the onset of necking. The mean values presented have been calculated for the batches V_0, H_0, C as well as for the batches V_1 and V_2, H_1 and H_2, X_1 and X_2 since these two batches respectively show a very similar characteristic. With respect to elastic deformation, which is represented by the ordinate intercept in Fig. 3, hybrid and conventional samples behave very similarly thus leading to the low $R_{p0.2}$ values of the hybrid samples. However, the plastic deformation behavior of the hybrid samples is a mix between the characteristic of the conventional (C) and the vertical batches (V_1, V_2): $\varepsilon_{max}(X_1 + X_2) = 22.9\%$ compared with the average $\varepsilon_{max} = 23.8\%$ for C and V_1, V_2, and $\sigma_{max}(X_1 + X_2) = 748.5$ MPa compared with the average $\sigma_{max} = 745.5$ MPa for C and V_1, V_2. Furthermore, a very distinct behavior between additively and conventionally processed SS 316L can be observed in the data. While the graph of conventional samples represents a ductile material response with large plastic strain ($\varepsilon = 35.2\%$), the ones of SLM processed tensile bars show more brittle material characteristics ($\varepsilon_{max} = 19.0\%$). However, even among the SLM processed batches an interesting trend can be noted: while the SLM process interruption leads to a drop of the maximum true stress that the samples can withstand before necking, it positively affects the maximum plastic strain. A further important result visualized in Fig. 3 is that horizontal samples with process interruption (H_1, H_2) can endure the same true stress as vertical samples manufactured with the standard SLM process (V_0).

3.3 Fractography

Based on representative fracture surfaces and cross sections of tensile bars Fig. 4, Fig. 5 and Fig. 6 give an overview of the various locations and potential reasons for failure of the tensile bars in dependence on their manufacturing process routes. Figure 4 displays etched cross sections of two vertically orientated tensile bars. The SLM process interruption was determined by the multiple melt pool boundaries at the same position in z direction. While the interruption presented in image (a) was not the initiation of failure, in image (b) and (c) the opposite is shown: failure that occurred in direct vicinity of the interruption, even though with the two-dimensional image of

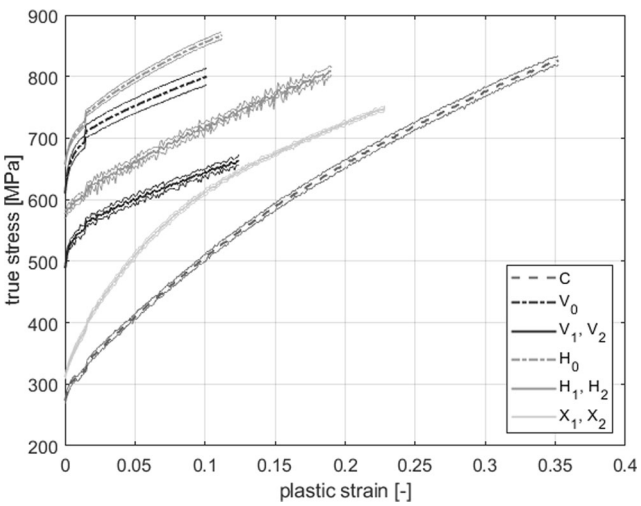

Fig. 3 True stress-plastic strain curves for various batches of tensile bars for the regions of uniform elongation. The end of the curves marks the onset of necking. For each batch the mean value ± standard deviation is displayed

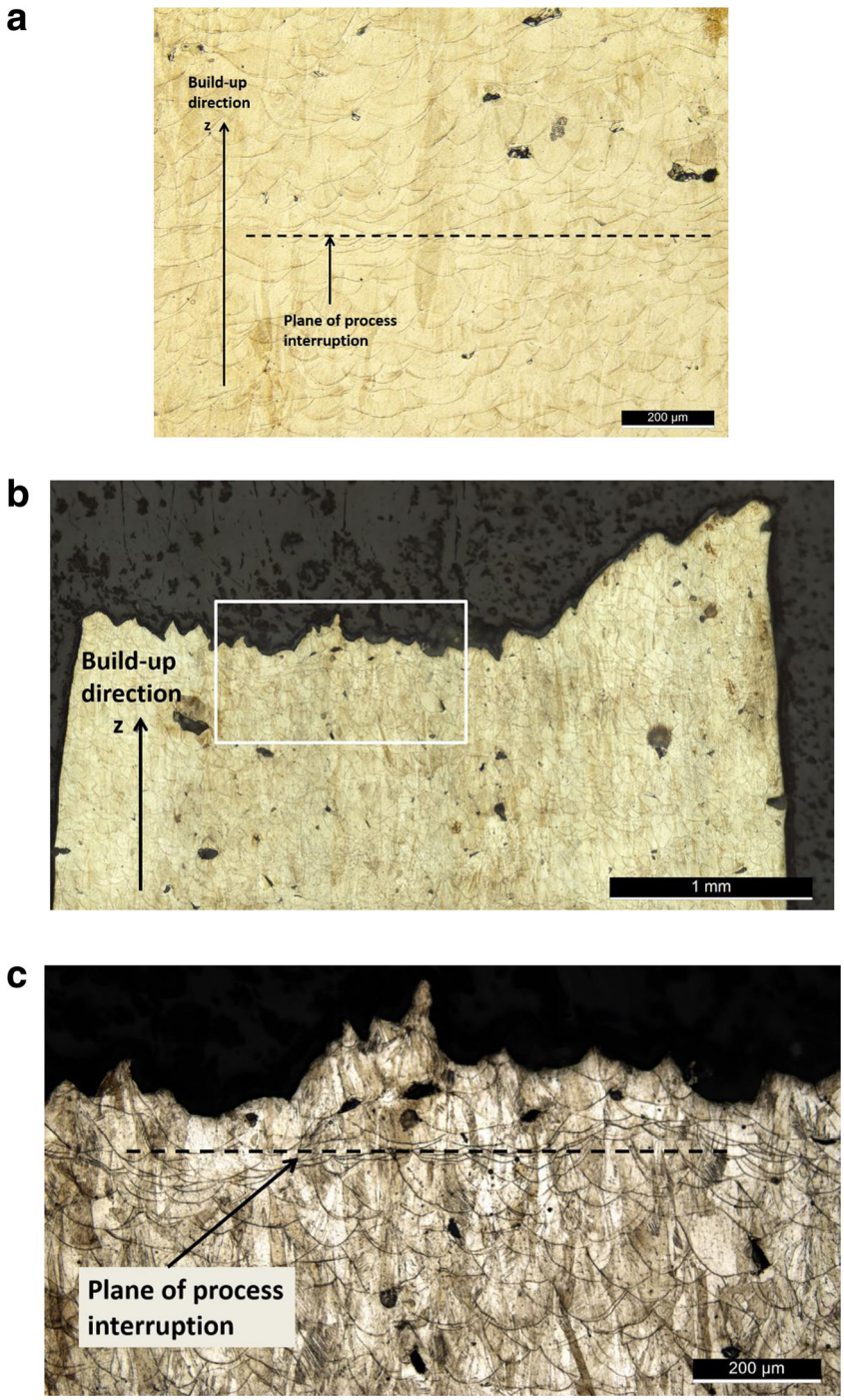

Fig. 4 Detection of level of SLM process interruption based on optical microscope images of etched cross sections of vertical tensile bars. **a** Sample of batch V_2—interruption level is not causing fracture. **b** Sample of batch V_2—fracture occurs in direct vicinity of the interruption level. **c** Detail of (**b**)

the cross section it is not possible to identify the exact location of the initiation of failure in the interruption plane. Although the data in Fig. 2 and Table 2 show the decrease of $R_{p0.2}$ and R_m as a consequence of SLM process interruption, the presence of both these cases (Fig. 4) indicates that the location of failure is not necessarily determined by the process interruption itself. However, the fracture surfaces of the vertical tensile bars depicted in Fig. 5 give an indication for both the decrease of strength and the location of rupture subsequently to a SLM process interruption. The detailed views of Fig. 5 b, d reveal each exemplarily one of the lacks of fusion present in Fig. 5 a, c. These lacks of fusion are irregularly formed defects. According to Zhang [18], they can result from a poor powder layer quality. For the experiment discussed here, the powder has partially been removed from the build plate and been refilled prior to the SLM process restart to adapt the process interruption during the manufacturing of the tensile bars as close as possible to the process of sensor integration into

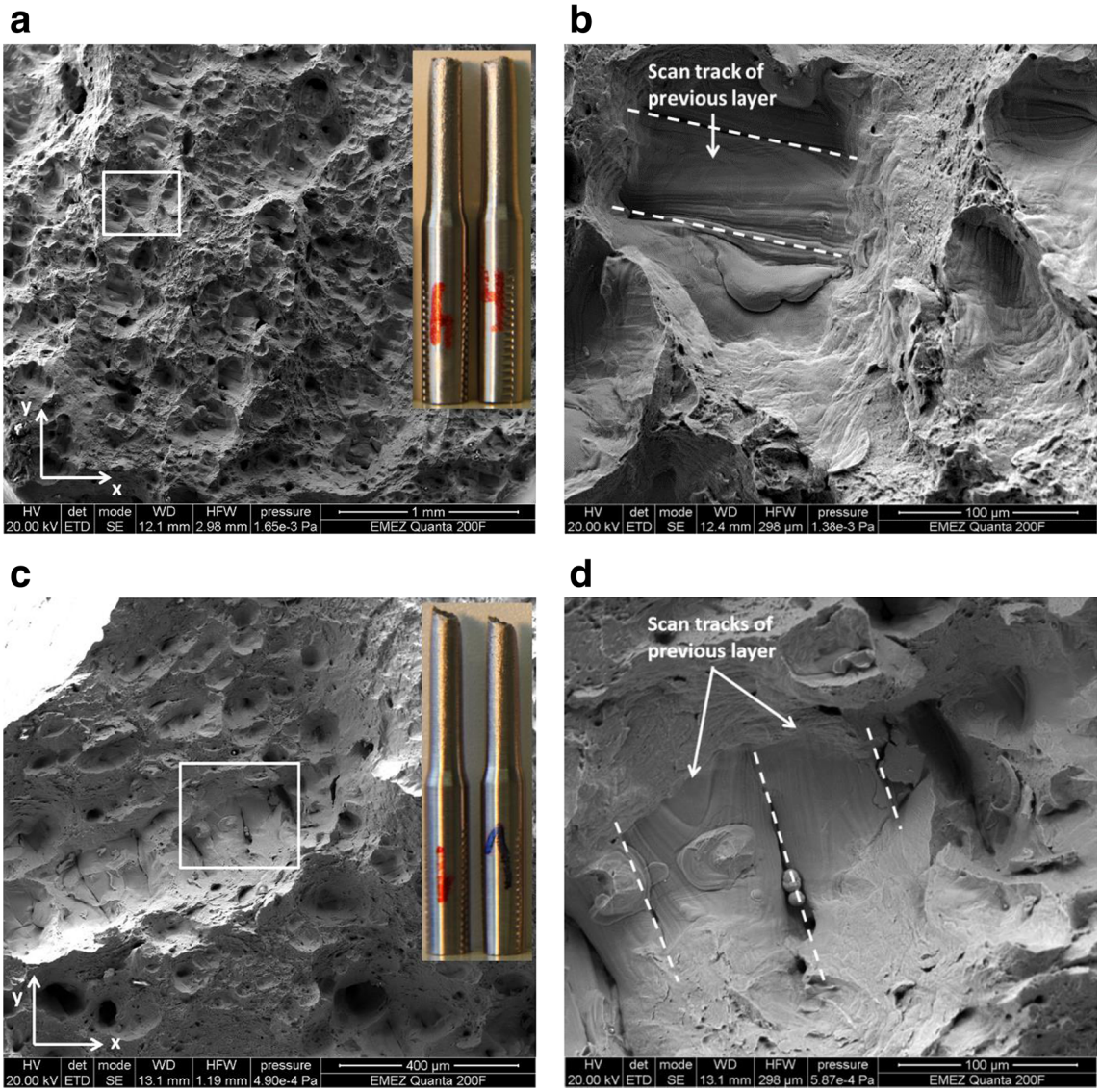

Fig. 5 **a** Tensile bar of batch V_2, **c** tensile bar of batch V_1—SEM images of fracture surfaces revealing lacks of fusion causing insufficient bonding, thus weakening the cross sections; tensile bars furthermore show the locations of failure. **b** Detail of (**a**). **d** Detail of (**c**)

SLM parts. This procedure negatively affected the homogeneity of the powder layer. Consequently, the process interruption increases the probability of occurrence of lacks of fusion thus causing a weak bonding between two layers leading to a failure of the tensile bars.

Subsequently to the discussion of the reasons and mechanisms of failure for tensile bars manufactured with SLM process interruption, the results of the hybrid samples are investigated based on a specimen indicating a representative behavior. Figure 6 b visualizes both the transition zone from turned part to SLM part and the location of failure very well. If the energy and heat input into the transition zone is sufficiently high, it is possible to achieve a connection that is not the weakest zone within the tensile bar (Fig. 6 c). Figure 6 a shows the fracture surface of the same tensile bar. Regarding the location of failure, it has to be stated that for the hybrid batches X_1, X_2 fracture occurred randomly, i.e., some tensile bars failed in the SLM part while others failed in the conventional section. The plastic deformation behavior of additively and conventionally processed SS 316L (Fig. 3) reveals similar values for true stress of these two materials (σ_{max} $(C) =$ 826 MPa; σ_{max} $(V_0) = 800$ MPa) indicating that they are not as different in their characteristic as it seemed from the data in Fig. 2 and Table 2. However, it has to be noted that the plastic deformation in this paper is only calculated in the uniform elongation regime and therefore does not allow to draw direct conclusions on the location of failure. Furthermore, it is mentionable that in the particular case of Fig. 6 b the transition zone represents a constraint for necking, but since this phenomenon cannot be observed for all hybrid tensile bars, a systematic behavior cannot be concluded.

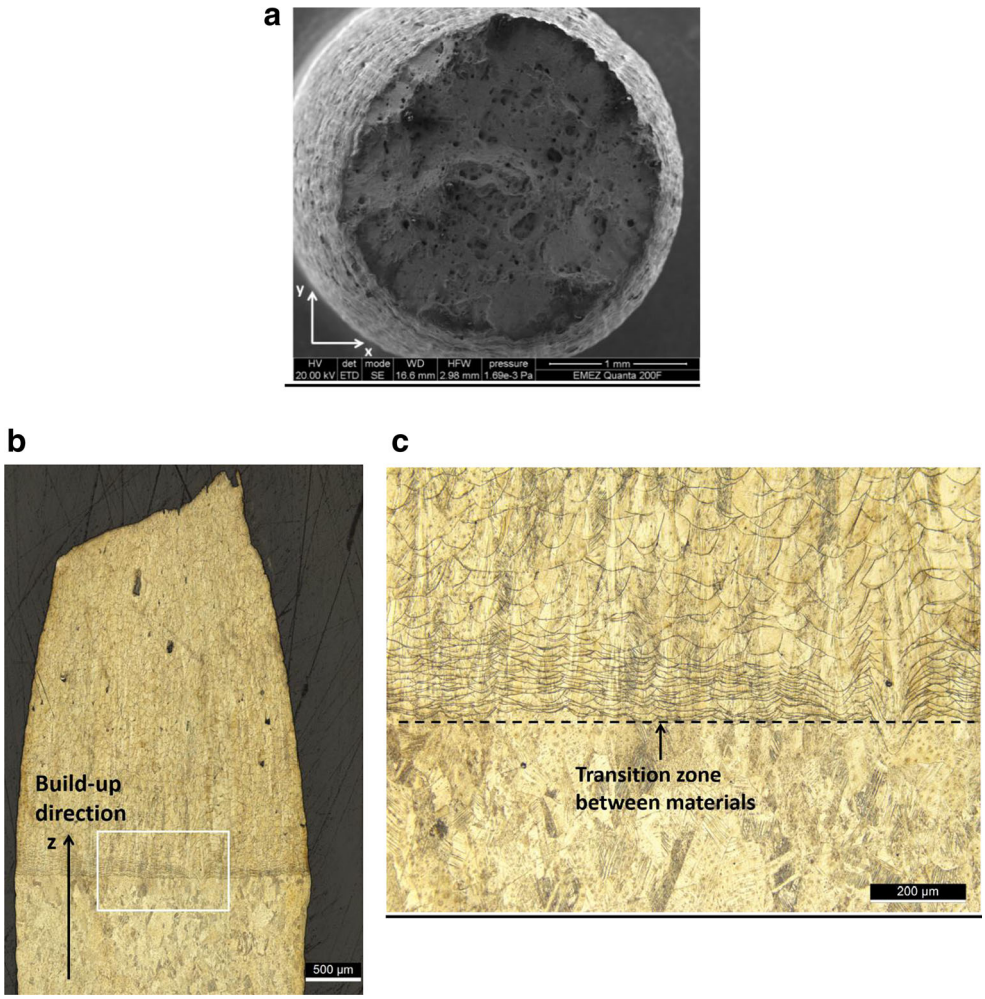

Fig. 6 Hybrid tensile bar. **a** SEM image of fracture surface. **b** Optical microscope image showing location of failure in relation to the transition zone for the same tensile bar as in (**a**). **c** Detail of (**b**)

Besides the temperature inhomogeneity as well as the negatively affected powder layer quality for samples manufactured in two steps (hybrid parts or parts with SLM process interruption), oxidation of the surfaces on which the process is continued later on needs to be taken into consideration. Although the oxidation phenomena have not been investigated in this paper, literature gives some important indications on its influence. Simonelli [19] reported on an experiment with an O_2 content of 0.2% in the process chamber which still led to oxidation of SS 316L samples during the SLM process. Hence, it is a valid assumption that an additional contact of the SLM samples with ambient air during a process interruption has no further detrimental impact on the mechanical properties. The machine used for the experiment presented in this paper is set to a maximum O_2 content of 0.3%. Certainly, the oxidation phenomenon also occurs on the surface of the conventionally manufactured lower halves of the hybrid tensile bars but because of the aforementioned literature results negative consequences on mechanical properties are not expected.

In addition to the discussion of the location of failure of the hybrid tensile bars, Fig. 6 b, c show another interesting and characteristic effect of the start of the SLM process. The nominal layer thickness, which is a predefined machine parameter (30 µm for the experiment in this paper), is not reached in the first layers. Instead, this nominal value is reached asymptotically after several layers have been built. The reason for this behavior is the powder layer density which is assumed to be in the range of 50%. Consequently, the consolidated material has an effective thickness of just 50% of the applied powder layer thickness, i.e., in this case a 30-µm thick powder layer results in a 15-µm thick layer of consolidated material. This effect is present for the first layers of each SLM built job until the nominal layer thickness of consolidated material is reached asymptotically. For the given assumptions, this transient oscillation of the layer thickness takes about 10 layers.

4 Conclusions and outlook

The investigations presented in this paper show that the tensile properties $R_{p0.2}$ and R_m of SLM manufactured parts decrease if the process contains a discontinuity like an interruption or if it starts within the final part's shape as it is the case for hybrid

samples. This is an important result which has to be taken into consideration for dimensioning parts containing any of the aforementioned discontinuities in the SLM manufacturing process. The decrease in the mechanical properties is more pronounced for vertically orientated specimens. In contrast to the influence of the process discontinuity on mechanical data, the way of SLM process restart or the pre-processing of the conventionally manufactured halves of the hybrid tensile bars has, at least in the way it has been varied and investigated in this study, no impact on the resulting tensile properties. The plastic deformation curves reveal that the hybrid tensile bars represent an even mix between the conventional and the additive material data, i.e., none is dominant. Regarding process interruption, it has to be stated that horizontal samples that have been built with a SLM process interruption can withstand the same true stress as vertically orientated ones that have been manufactured in one step. The location of failure has a random distribution for the batches of hybrid tensile bars, which means it can occur either in the SLM or in the conventional part. Consequently, the process discontinuity as such is not determining the location of failure. This can also be observed for the additively processed horizontal batches. For the vertical samples, the fracture occurs in various regions of the gage length, but the fractographic analysis (Fig. 5) also shows that the process interruption raises the probability of occurrence of bonding defects which weaken that cross section. Since for the vertical samples the load during tensile testing is applied perpendicular to the plane of process interruption, the probability of failure in that cross section raises.

Finally, it has to be stated that the results presented in this paper are very important for the industrial sectors planning to enter the field of sensor/actuator embedding as well as the industries aiming at manufacturing hybrid parts. The paper reports new material data that is crucial for precise dimensioning of workpieces manufactured according to aforementioned processing routes. However, these results are just the first step in investigating these non-standard processing routes and their impact on material properties. Based on this, further material data has to be acquired to get a deeper understanding of the effects present during a process discontinuity.

Acknowledgements The authors like to thank the Swiss Commission for Technology and Innovation (CTI) for financing the analysis within the frame of a founded project. Furthermore, special thanks go to Mrs. Chiara Bertoli (Institute for Virtual Manufacturing IVP, ETH Zurich) who supported the authors in a very patient way with her expertise in plastic material deformations.

Compliance with ethical standards

Conflict of interest The authors declare that they have no conflict of interest.

References

1. Paz JFI, Wilbig J, Aumund-Kopp C, Petzoldt F (2014) RFID transponder integration in metal surgical instruments produced by additive manufacturing. 57:365–372. https://doi.org/10.1179/1743290114Y.0000000112
2. Sehrt J, Witt, G. Additive manufacturing of smart parts and medical instruments
3. Stoll P, Leutenecker-Twelsiek B, Spierings A, Klahn C, Wegener K (2018) Temperature monitoring of an SLM part with embedded sensor. In: Cham (ed) Industrializing additive manufacturing - proceedings of additive manufacturing in products and applications - AMPA2017. Springer International Publishing, pp 273–284
4. Li X (2001) Embedded sensors in layered manufacturing. Dissertation, Stanford University,
5. Maier RRJ, Havermann D, MacPhseron WN, Hand DP (2013) Embedding metallic jacketed fused silica fibres into stainless steel using additive layer manufacturing technology. In: Jaroszewicz LR (ed) Fifth European workshop on optical fibre sensors. SPIE Proceedings, p 4. https://doi.org/10.1117/12.2026076
6. Havermann D, Mathew J, MacPherson WN, Maier RRJ, Hand DP (2015) Temperature and strain measurements with fiber Bragg gratings embedded in stainless steel 316. J Lightwave Technol 33(12):2474–2479
7. Havermann D, Mathew J, MacPherson WN, Maier RR (2014) Hand DP in-situ measurements with fibre Bragg gratings embedded in stainless steel. Proc SPIE:9157A9151-9157A9151
8. Stoll P, Mathew J, Spierings A, Bauer T, Maier RRJ, Wegener K (2016) Embedding fibre optical sensors into SLM parts. In: 27th annual international solid freeform fabrication symposium - an additive manufacturing conference, Austin
9. Haba AG, Haba INOX V4A Datasheet
10. Spierings AB, Schneider M, Eggenberger R (2011) Comparison of density measurement techniques for additive manufactured metallic parts. 17(5):380–386. https://doi.org/10.1108/13552541111156504
11. Levy GN, Schindel R, Kruth JP (2003) Rapid manufacturing and rapid tooling with layer manufacturing (LM) technologies, state of the art and future perspectives. CIRP Ann 52(2):589–609. https://doi.org/10.1016/S0007-8506(07)60206-6
12. Mertens A, Reginster S, Contrepois Q, Dormal T, Lemaire O, Lecomte-Beckers J (2014) Microstructures and mechanical properties of stainless steel AISI 316L processed by selective laser melting. 783-786. https://doi.org/10.4028/www.scientific.net/MSF.783-786.898
13. Mower TM, Long MJ (2016) Mechanical behavior of additive manufactured, powder-bed laser-fused materials. Mater Sci Eng A 651:198–213. https://doi.org/10.1016/j.msea.2015.10.068
14. Riemer A, Leuders S, Thöne M, Richard HA, Tröster T, Niendorf T (2014) On the fatigue crack growth behavior in 316L stainless steel manufactured by selective laser melting. Eng Fract Mech 120:15–25. https://doi.org/10.1016/j.engfracmech.2014.03.008
15. Spierings A, Herres N, Levy G (2011) Influence of the particle size distribution on surface quality and mechanical properties in AM steel parts, vol 17. https://doi.org/10.1108/13552541111124770
16. Hitzler L, Hirsch J, Heine B, Merkel M, Hall W, Öchsner A (2017) On the anisotropic mechanical properties of selective laser-melted stainless steel. Materials 10(10):1136. https://doi.org/10.3390/ma10101136
17. Merkt S (2015) Qualifizierung von generativ gefertigten Gitterstrukturen für massgeschneiderte Bauteilfunktionen. Dissertation, RWTH Aachen,

18. Zhang B, Li Y, Bai Q (2017) Defect formation mechanisms in selective laser melting: a review. Chin J Mech Eng 30(3):515–527. https://doi.org/10.1007/s10033-017-0121-5
19. Simonelli M, Tuck C, Aboulkhair N, Maskery I, Wildman R, Hague R (2015) A study on the laser spatter and the oxidation reactions during selective laser melting of 316L stainless steel, Al-Si10-Mg, and Ti-6Al-4V, vol 46. https://doi.org/10.1007/s11661-015-2882-8